DOI: 10.1007/s12541-012-0188-y

# Experiment-Based Design Optimization of a Washing Machine Liquid Balancer for Vibration Reduction

**Seok-Ho Son[1], Sang-Bin Lee[2], and Dong-Hoon Choi[1,#]**

1 School of Mechanical Engineering, Hanyang University, 17, Haengdang-dong, Seongdong-gu, Seoul, South Korea, 133-791
2 Samsung Electronics Co. Ltd., 416, Maetan 3-dong, Yeongtong-gu, Suwon, Gyeonggi-do, South Korea, 433-742
# Corresponding Author / E-mail: dhchoi@hanyang.ac.kr, TEL: +82-2-2220-0478, FAX: +82-2-2291-4070

KEYWORDS: Washing machine, Liquid automatic balancer, Optimization, Meta-model

*The most prevalent problem in washing machines is the vibration incurred during the spin cycles. The balance of the washing machine plays an important role in reducing the vibrations from an unbalanced mass by injecting salt water into an automatic balancer. In this study, we determined the optimal dimension of layers and the amount of salt water for an automatic liquid balancer in order to minimize the maximum displacement of a low-speed spin cycle while satisfying the design constraint on the maximum displacement of a high-speed spin cycle. The maximum displacements for a specified design point were obtained by performing laboratory experiments. For design optimization, approximate models of the maximum displacements were created by employing radial basis function regression (RBFr) models based on the experimental data at full factorial design points. Then, an optimization algorithm was applied to the RBFr models to obtain the optimum solution. Using the proposed design approach, the optimal value of the maximum displacement of a low-speed spin cycle was reduced by 13.1%, compared to the initial value, while satisfying the design constraint on the maximum displacement of a high-speed spin cycle.*

Manuscript received: August 31, 2011 / Accepted: March 14, 2012

## 1. Introduction

There are two types of washing machines -- front-loading or drum types and top-loading types. The front-loading washer is mostly used in Europe while the top-loading washer is very popular in Asia. The top-loading washing machine can be further classified two subtypes -- an automatic washing machine, shown in Fig. 1(b), and a semi-auto washing machine, shown in Fig. 1(c).

Yet, for all types of washing machines, vibration and noise negatively affect the lifetime and reliability of the operation and capacity of the machine.[1] Although the vibration of a washing machine occurs mostly when the laundry is washed and dewatered, the spinning process during dewatering is more critical than the washing process because the spinning process has a higher rotational speed.[2,3] The twisting and crumpling of the laundry during dewatering results in an unbalanced mass that induces vibrations. These vibrations can be reduced to a small degree by bellows in the spin component; however, to reduce the vibrations most effectively, installation of an automatic balancer on top of the spin component is necessary.[3] The automatic balancer uses balls or a liquid similar to salt water to create motion in the direction that will most neutralize the vibrations within a tube of the balancer.

Recently, much research has been focused on automatic balancers. For example, Wlerzba et al.[4] developed a ball balancer for vibration reduction, and Kang et al.[5] studied the fluid drag force on a ball balancer. There has also been extensive research on liquid balancers. Oh et al.[3] modeled the dynamics of a washing machine system with an automatic balancer and demonstrated its performance using both experimental and computational analysis. Leonardo-Sot et al.[6] proposed a dynamic model with two degrees of freedom (DOF) using a Leblanc balancer that described two waves: one was synchronous with the rigid body motion while the other was a backward traveling wave. In another set of experiments, Jung et al.[7] researched the technical difficulties and solutions for a washing machine at two stages. In addition, Chen et al.[8] studied the effects of a hydraulic balancer and proved the existence of an unstable region through simulation and experiment. Bae et al.[9] researched the effects of a variety of parameters on the vibration of a washing machine using a numerical method and proposed a design to improve the machine's performance.

Although many researchers have dynamically modeled and analyzed washing machines with automatic balancers and have proposed improved designs, no report exists (to the authors' knowledge) on the design optimization of a liquid automatic

(a) Front-loading (b) Auto top-loading (c) Semi-auto top-loading

Fig. 1 Types of washing machines

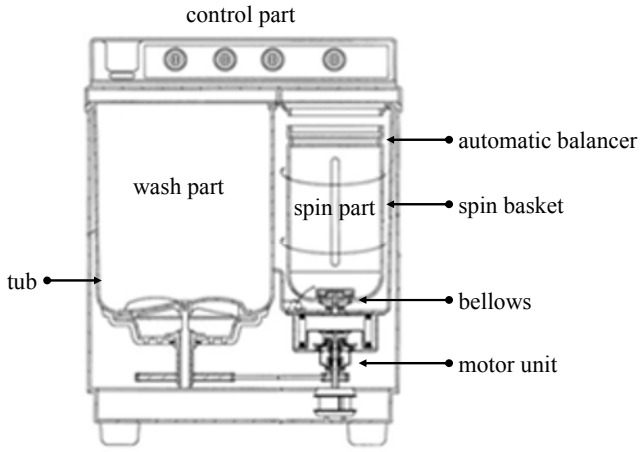


Fig. 2 The structure of the semi-automatic washing machine used in this study

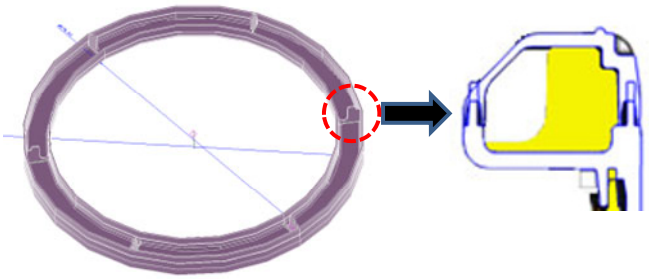

Fig. 3 An automatic liquid balancer

balancer for vibration reduction of a washing machine using numerical optimization techniques. In this study, we determined the optimal dimension of layers and amount of salt water necessary for an automatic liquid balancer to minimize the maximum displacement of a low-speed spin cycle while satisfying the design constraint on the maximum displacement of a high-speed spin cycle. The automatic liquid balancer for this study was installed in a semi-automatic washing machine, which was composed of both wash and spin components, as shown in the Fig. 2. The spin component was composed of dewatering equipment, including a spin basket, a motor unit, and an automatic balancer. The spin basket was connected to the bellows and allowed for 3-D rigid body motion. The automatic liquid balancer was filled with salt water and had six equally-spaced layers, as shown in Fig. 3. Note that the vibration reduction ability of the automatic balancer was known from previous research to depend on the shape of the layers and the amount of salt water.

## 2. Design Problem Formulation

The vibration caused by an unbalanced mass has a strong effect on the washing machine at lower RPMs (or an early spinning stage) because the washing machine passes through a resonant RPM at lower RPMs. At higher RPMs, even if the unbalanced mass is balanced by the automatic balancer, vibration occurs due to the centrifugal force of the rotating spin basket. Thus, we want to minimize the vibrations at lower RPMs while keeping the vibrations at higher RPMs within an allowable range. Note that, in this study, we quantified the amount of vibration of the machine by the maximum displacement of the spin component. Hence, we formulated a design optimization problem that minimized the maximum displacement of the spin component at a lower RPM while satisfying the design constraint on the maximum displacement of the spin component at a higher RPM. The dimension of the layers positioned in the balancer and the amount of salt water inside the balancer were selected as design variables.

Design optimization requires an analysis procedure whereby the responses of interest are evaluated for a specified design point. In this study, the responses of interest were evaluated by performing laboratory experiments as described in the next section. Then, to obtain an optimal design result using the experimental data, we adopted the strategy of meta-model-based design optimization. For this method, a design of experiments (DOE), meta-modeling, and an optimization algorithm are sequentially applied. The DOE, meta-modeling, and optimization algorithm employed in this study are presented in Sections 4.1, 4.2, and 4.3, respectively.

Denoting the meta-models of the maximum displacements at lower RPMs and higher RPMs as $\tilde{D}_{lower}$ and $\tilde{D}_{higher}$, respectively, our design problem can be formulated as

$$\text{Find} \quad \mathbf{x} \tag{1}$$

$$\text{to minimize} \quad \tilde{D}_{lower}(\mathbf{x}) \tag{2}$$

$$\text{satisfying} \quad \tilde{D}_{higher}(\mathbf{x}) \le \delta, \quad \mathbf{x}^{\mathrm{L}} \le \mathbf{x} \le \mathbf{x}^{\mathrm{U}} \tag{3}$$

where $\mathbf{x}$ is a vector of design variables, and superscripts L and U are the lower and upper limit values, respectively. In Eq. (3), $\delta$ is the allowable displacement.

## 3. Experimental Analysis

In this study, the responses of interest, the maximum displacements at lower and higher RPMs, were obtained by carrying out laboratory experiments. At the top of the spin basket, the displacement is almost always highest within our operating range. Thus, we measured the displacement at the top of the spin basket. The same washing machine was used for all of the experiments, but the liquid balancer was changed in order to obtain data showing only the design change effect of the liquid balancer. To impose consistent loading, the same artificial unbalanced mass

Fig. 4 Maximum displacement measurement using a super-high speed camera

was set at the same position for each experiment. Then, the experiments were conducted five times for each design and the average was taken to be the response value of interest. This process was employed to reduce the effect of random experimental error.

The procedure of measuring the responses of interest -- the maximum displacements at lower and higher RPMs -- using a super-high speed camera is as follows:

1. Install a super-high speed camera to film the spin component where an artificial unbalanced mass is attached, as shown in the left photo of Fig. 4.
2. Record the vibrations of the spin component using the super-high speed camera until the rotational speed of the spin component reaches the maximum value.
3. Transfer the recorded video file to a personal computer to measure the maximum displacements.
4. Find the video frames that show the vibrations of the spin component at the lower and higher RPM settings.
5. Measure the difference between the initial position and the maximally displaced position in each video frame using measurement software, as shown in the right photo of Fig. 4. These differences represent the maximum displacements at the lower and higher RPMs.

## 4. Optimization Strategy

To effectively implement the meta-model-based design optimization, a commercial process integration and design optimization (PIDO) software, PIAnO,[10] was employed in this study.

### 4.1 Design of Experiments

The design of experiments (DOE) process is a scientific approach to planning experiments that allows one to conduct the experiments most efficiently and then to analyze the system using statistical methods. The DOE is often used to determine which design variables (or factors) have significant influence on a response variable (or a characteristic variable), and thus, which design variables should be selected to achieve the best solution.

There are a variety of methods for locating the experimental points including full factorial design (FFD), fractional factorial design, central composite design (CCD), and Box-Behnken design (BBD) methods. In this study, we adopted the $3^3$ design method, which utilizes three factors (or three design variables) at three different levels arranged in a factorial experiment.[11,12] Twenty-seven factor combinations are shown in Fig. 5 and listed in Table 1. To reduce the effect of random experimental error, we conducted experiments at each factor combination five separate times and then took the average to be the maximum displacement for the low- and high-RPM settings, as described in Section 3. Experimental results scaled by the minimum value at each RPM setting are also listed in Table 1.

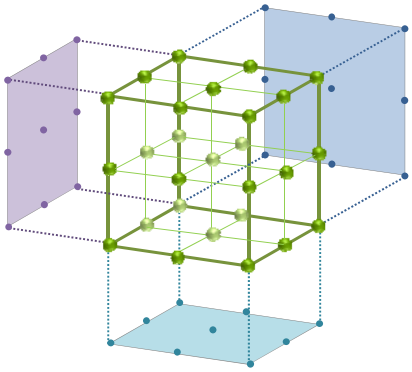

Fig. 5 Experimental layout of the $3^3$ design

Table 1 27 Factor combinations and experimental results

| | | | | Maximum Displacement at a lower RPM | | | | | | Maximum Displacement at a higher RPM | | | | | |
|---|---|---|---|---|---|---|---|---|---|---|---|---|---|---|---|
| NO | Width | Height | Salt Water | #1 | #2 | #3 | #4 | #5 | AVR | #1 | #2 | #3 | #4 | #5 | AVR |
| 1 | -1 | -1 | -1 | 1.067 | 1.026 | 1.000 | 1.026 | 1.062 | 1.036 | 1.314 | 1.373 | 1.275 | 1.333 | 1.373 | 1.333 |
| 2 | -1 | -1 | 0 | 1.077 | 1.128 | 1.077 | 1.077 | 1.077 | 1.087 | 1.216 | 1.373 | 1.353 | 1.373 | 1.412 | 1.345 |
| 3 | -1 | -1 | 1 | 1.103 | 1.051 | 1.087 | 1.067 | 1.077 | 1.077 | 1.333 | 1.275 | 1.275 | 1.373 | 1.275 | 1.306 |
| 4 | -1 | 0 | -1 | 1.221 | 1.215 | 1.241 | 1.231 | 1.246 | 1.231 | 1.392 | 1.373 | 1.353 | 1.373 | 1.373 | 1.373 |
| 5 | -1 | 0 | 0 | 1.113 | 1.103 | 1.118 | 1.097 | 1.077 | 1.102 | 1.333 | 1.412 | 1.392 | 1.373 | 1.373 | 1.376 |
| 6 | -1 | 0 | 1 | 1.287 | 1.292 | 1.292 | 1.282 | 1.272 | 1.285 | 1.529 | 1.667 | 1.569 | 1.627 | 1.569 | 1.592 |
| 7 | -1 | 1 | -1 | 1.328 | 1.374 | 1.359 | 1.338 | 1.333 | 1.347 | 1.275 | 1.333 | 1.353 | 1.275 | 1.314 | 1.310 |
| 8 | 0 | 1 | 0 | 1.262 | 1.256 | 1.282 | 1.256 | 1.292 | 1.270 | 1.333 | 1.216 | 1.196 | 1.255 | 1.275 | 1.255 |
| 9 | 0 | 1 | 1 | 1.385 | 1.369 | 1.374 | 1.385 | 1.359 | 1.374 | 1.412 | 1.373 | 1.392 | 1.353 | 1.333 | 1.373 |
| 10 | 0 | -1 | -1 | 1.256 | 1.287 | 1.292 | 1.277 | 1.282 | 1.279 | 1.020 | 1.039 | 1.000 | 1.059 | 1.039 | 1.031 |
| 11 | 0 | -1 | 0 | 1.277 | 1.282 | 1.272 | 1.231 | 1.282 | 1.269 | 1.137 | 1.137 | 1.176 | 1.157 | 1.176 | 1.157 |
| 12 | 0 | -1 | 1 | 1.205 | 1.179 | 1.169 | 1.221 | 1.179 | 1.191 | 1.176 | 1.137 | 1.078 | 1.137 | 1.176 | 1.141 |
| 13 | 0 | 0 | -1 | 1.621 | 1.615 | 1.641 | 1.631 | 1.641 | 1.630 | 1.392 | 1.373 | 1.333 | 1.353 | 1.392 | 1.369 |
| 14 | 0 | 0 | 0 | 1.595 | 1.579 | 1.590 | 1.590 | 1.585 | 1.588 | 1.333 | 1.373 | 1.392 | 1.373 | 1.353 | 1.365 |
| 15 | 0 | 0 | 1 | 1.590 | 1.600 | 1.590 | 1.595 | 1.595 | 1.594 | 1.353 | 1.373 | 1.373 | 1.392 | 1.373 | 1.373 |
| 16 | 0 | 1 | -1 | 1.179 | 1.169 | 1.231 | 1.221 | 1.210 | 1.202 | 1.392 | 1.373 | 1.333 | 1.392 | 1.392 | 1.376 |
| 17 | 0 | 1 | 0 | 1.231 | 1.277 | 1.231 | 1.262 | 1.256 | 1.251 | 1.196 | 1.255 | 1.176 | 1.196 | 1.216 | 1.208 |
| 18 | 0 | 1 | 1 | 1.426 | 1.415 | 1.379 | 1.385 | 1.395 | 1.400 | 1.510 | 1.471 | 1.353 | 1.412 | 1.373 | 1.424 |
| 19 | 1 | -1 | -1 | 2.056 | 2.026 | 2.036 | 2.041 | 2.021 | 2.036 | 2.784 | 2.843 | 2.863 | 2.882 | 2.824 | 2.839 |
| 20 | 1 | -1 | 0 | 1.974 | 1.995 | 2.005 | 1.944 | 1.969 | 1.977 | 2.118 | 2.176 | 2.196 | 2.137 | 2.235 | 2.173 |
| 21 | 1 | -1 | 1 | 1.872 | 1.851 | 1.856 | 1.836 | 1.831 | 1.849 | 1.922 | 1.980 | 1.882 | 1.863 | 1.902 | 1.910 |
| 22 | 1 | 0 | -1 | 1.692 | 1.682 | 1.692 | 1.687 | 1.641 | 1.679 | 1.333 | 1.216 | 1.235 | 1.275 | 1.353 | 1.282 |
| 23 | 1 | 0 | 0 | 1.538 | 1.559 | 1.569 | 1.538 | 1.569 | 1.555 | 1.373 | 1.314 | 1.392 | 1.392 | 1.431 | 1.380 |
| 24 | 1 | 0 | 1 | 1.538 | 1.528 | 1.538 | 1.533 | 1.538 | 1.535 | 1.235 | 1.216 | 1.275 | 1.255 | 1.235 | 1.243 |
| 25 | 1 | 1 | -1 | 1.518 | 1.538 | 1.528 | 1.538 | 1.533 | 1.531 | 1.275 | 1.255 | 1.333 | 1.235 | 1.216 | 1.263 |
| 26 | 1 | 1 | 0 | 1.533 | 1.518 | 1.528 | 1.538 | 1.544 | 1.532 | 1.196 | 1.176 | 1.196 | 1.137 | 1.157 | 1.173 |
| 27 | 1 | 1 | 1 | 1.523 | 1.533 | 1.538 | 1.533 | 1.538 | 1.533 | 1.333 | 1.333 | 1.294 | 1.373 | 1.353 | 1.337 |

To examine the accuracy of our experiment method, we calculated the coefficient of variation (CV) among five repeated experiment results at each factor combination. The CVs for the maximum displacement at a lower RPM and at a higher RPM were found to range between 0.2% and 2.4% and between 0.9% and 5.0%, respectively, which confirms the accuracy of our experiment method.

### 4.2 Meta-modeling

Meta-modeling is the process of creating an approximate continuous function using a discrete set of data. There are two kinds of meta-models: regression models and interpolation models. We chose a regression model to approximate the maximum displacements in order to smooth out the random errors contained in the 27 experimental results listed in Table 1.

In this study, we generated three popular regression models: a full quadratic polynomial regression (PR) model, a simple cubic PR model, and a radial basis function regression (RBFr) model. Then,

we compared the accuracy of each model and selected the regression model with the best accuracy for each response of interest.

Since PR models are well known, only the RBFr model will be briefly described here. The RBFr model $\tilde{y}(\mathbf{x})$ predicts the $y$ value at a design point $\mathbf{x}$ by taking the inner product of a vector of $m$ basis functions ($\mathbf{h}(\mathbf{x})$) and a vector of $m$ weights ($\mathbf{w}$), as formulated in Eq. (4).[13-16]

$$\tilde{y}(\mathbf{x}) = \mathbf{h}^t(\mathbf{x})\mathbf{w} \tag{4}$$

where

$$\mathbf{h}(\mathbf{x}) = \left[\mathrm{h}_1(\mathbf{x}) \quad \mathrm{h}_2(\mathbf{x}) \quad \cdots \quad \mathrm{h}_m(\mathbf{x})\right]^t \tag{5}$$

In Eq. (4), the vector $\mathbf{w}$ can be evaluated by minimizing the residual sum of the squares, as formulated in Eq. (6):

$$\text{minimize} \quad \boldsymbol{\varepsilon}^t\boldsymbol{\varepsilon} = \left(\mathbf{y}_{\exp} - \mathbf{H}\mathbf{w}\right)^t\left(\mathbf{y}_{\exp} - \mathbf{H}\mathbf{w}\right) \tag{6}$$

The least squares estimator for $\mathbf{w}$ is

$$\mathbf{w} = \left(\mathbf{H}^t\mathbf{H}\right)^{-1}\mathbf{H}^t\mathbf{y}_{\exp} \tag{7}$$

In Eqs. (6) and (7), $\mathbf{H}$ is a matrix of $m$ radial basis function values at $nexp$ sampling points, as shown in Eq. (8):

$$h_i(\mathbf{x}) = \exp\left(-\frac{\left|\mathbf{x}-\mathbf{x}_i\right|^2}{r^2}\right) \tag{8}$$

In this study, we chose the Gaussian function as the radial basis function[16] which can be expressed in term of Euclidean distance, as defined by Eq. (9):

$$h_i(\mathbf{x}) = \exp\left(-\frac{\left|\mathbf{x}-\mathbf{x}_i\right|^2}{r^2}\right) \tag{9}$$

where $r$ is a user-defined parameter.

To evaluate the accuracies of the three regression models that we chose, we utilized the coefficient of determination $R^2$, as defined in Eq. (10):

$$R^2 = 1 - \frac{\sum_{i=1}^{nexp}\left[y(\mathbf{x}_i) - \hat{y}(\mathbf{x}_i)\right]^2}{\sum_{i=1}^{nexp}\left[y(\mathbf{x}_i) - \bar{y}\right]^2} \tag{10}$$

where $y(\mathbf{x})$ and $\tilde{y}(\mathbf{x})$ denote an exact value and an approximate value, respectively. The closer the $R^2$ value is to 1, the more accurate a regression model is. We evaluated the $R^2$ values of three regression models (full quadratic PR, simple cubic PR, and RBFr) for the maximum displacements at a lower RPM and a higher RPM; the results are shown in Fig. 6 in %. For the low-RPM maximum displacement values (white bar in Fig. 6), all three models show the same $R^2$ value of about 93%. However, for the high-RPM maximum displacement values (black bar in Fig. 6), the $R^2$ value of the RBFr model is about 95% while the $R^2$ values of two PR models are about 67%. Thus, we used the RBFr model to analyze the maximum displacements for both the low-RPM and high-RPM experiments.

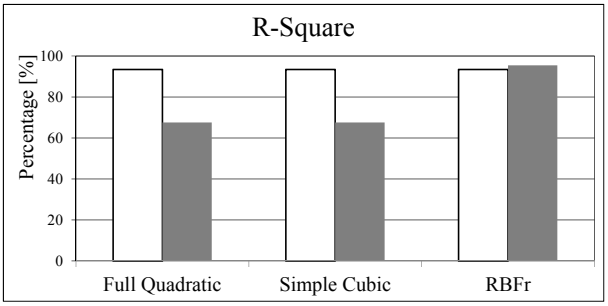


Fig. 6 $R^2$ values of three regression models

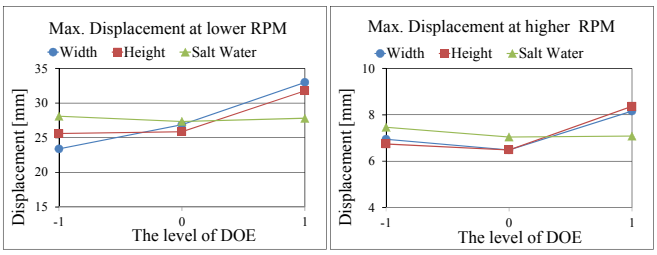


(a) (b)

Fig. 7 ANOM results for (a) the maximum displacement at a lower RPM and (b) the maximum displacement at a higher RPM

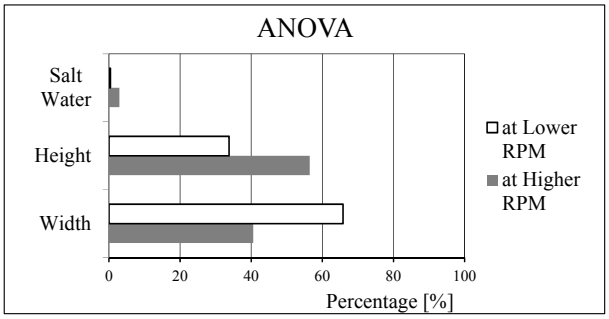


Fig. 8 ANOVA results

### 4.3 Optimization Algorithm

In order to obtain the results of the design optimization based on the meta-models, we integrated the RBFr model generated in Section 4.2 into an optimization algorithm in the PIAnO environment. For the optimization algorithm, we utilized an efficient gradient-based approximate optimization algorithm, called an enhanced two-point diagonal quadratic approximation method,[17] which is available in PIAnO.

## 5. Design Results

### 5.1 Effects of design variables on the responses of interest

To investigate the effects of the three design variables on the two responses of interest (the maximum displacements), we studied the analysis of means (ANOM) and the analysis of variance (ANOVA) using the 27 experimental data points sampled by the 3 levels of FFD. The results of the ANOM, shown in Fig. 7, and the ANOVA, shown in Fig. 8, indicate that the width and height of a layer have stronger influences on the maximum displacements than the amount of salt water, at both the low- and high-RPM settings.

Table 2 Results of optimization based on meta-models

| | | Lower | Initial | Optimal | Upper |
|---|---|---|---|---|---|
| Design variables | Width | 0 | 0.5 | 0.191 | 1 |
| | Height | 0 | 0.5 | 0.386 | 1 |
| | Salt Water | 0 | 0.5 | 0.123 | 1 |
| Objective | | | 1.0 | 0.881 | |
| Constraint | | | 0.93 | 1.000 | 1 |

Table 3 Results of the validation experiment

| | | Lower | Initial | Optimal | Upper |
|---|---|---|---|---|---|
| Design variables | Width | 0 | 0.5 | 0.200 | 1 |
| | Height | 0 | 0.5 | 0.386 | 1 |
| | Salt Water | 0 | 0.5 | 0.125 | 1 |
| Objective | | | 1.0 | 0.869 | |
| Constraint | | | 0.983 | 1.016 | 1 |

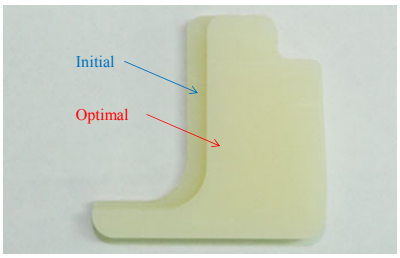


Fig. 9 Optimum and initial layers

### 5.2 Results of optimization based on meta-models

We successfully obtained optimization results using the meta-model-based design optimization described in Section 4. Table 2 lists the initial and optimal values of the three design variables, the objective function, and the constraint. Note that the design variable values are normalized between the lower limit value of 0 and the upper limit value of 1. Note also that objective values are scaled by the initial objective value, and the constraint values are scaled by the upper limit value. As shown in Table 2, the value of the objective function (the maximum displacement at a lower RPM) decreased by about 11.7% compared to its initial value while still satisfying the constraint on the high-RPM maximum displacement with the reduced values of all three design variables.

### 5.3 Validation experiment

In order to verify the validity of our meta-model-based design optimization results, we first adjusted the optimal design variable values to the values listed in Table 3 taking manufacturing into account and manufactured the layers according to the optimal design variable values listed in Table 3 and performed an additional experiment as described in Section 3. Photographs of the manufactured optimum and initial layers are shown in Fig. 9. The results of this validation experiment are listed in Table 3. As can be seen in Table 3, the objective value was found to decrease by about 13.1% while still satisfying the constraint, which verifies the validity of our meta-model based design optimization results.

Fig. 10 compares the scaled values of the objective function and constraint for the initial and optimal designs obtained by the experiment and the meta-models. This comparison indicates that the meta-models employed in this study are accurate enough to obtain an optimal solution.

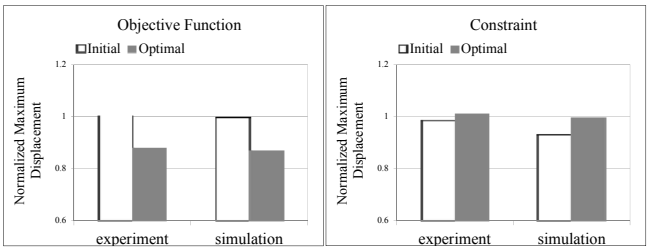


Fig. 10 Comparisons of the scaled objective and constraint values between the real experiment and the meta-models

## 6. Conclusions

In order to reduce the vibrations of a washing machine, we formulated a design optimization problem that minimized the maximum displacement of the spin component in a low-RPM setting while satisfying the design constraint on the maximum displacement of the spin component in a high-RPM setting. The width and height of the layers positioned in the balancer and the amount of salt water inside the balancer were selected as design variables. In this study, the maximum displacements of the low-RPM and high-RPM settings were obtained via laboratory experiments. Then, to determine the optimal design result using the experimental data, we employed meta-model-based design optimization, whereby a design of experiments (DOE), meta-modeling, and an optimization algorithm were sequentially applied.

We successfully obtained optimal results using the meta-model-based design optimization and performed an additional experiment to verify the validity of our results by installing optimally designed layers. The maximum displacement of the lower RPM was found to decrease about 13.1% compared to its initial value while still satisfying the constraint on the maximum displacement of the higher RPM.

We believe that the strategy of meta-model-based design optimization presented in this study can also be applied to a variety of design cases in which the responses of interest are evaluated by performing laboratory experiments.

## ACKNOWLEDGEMENT

This work was supported by a National Research Foundation of Korea (NRF) grant, funded by the Korea government (MEST) (No. 2011-0016701). The authors express gratitude to PIDOTECH, Inc. for providing the PIAnO software as a PIDO tool.

## REFERENCES

1. Nygards, T., “Washing Machine Design Optimization Based on Dynamics Modeling,” Ph.D. Thesis, Department of Applied Mechanics, Chalmers University of Technology, 2011.
2. Lim, H. T., Jeong, W. B., and Kim, K. J., “Dynamic Modeling

and Analysis of Drum-type Washing Machine," Int. J. Precis. Eng. Manuf., Vol. 11, No. 3, pp. 407-417, 2010.

3. Oh, H. J. and Lee, U. S., "Dynamic Modeling and Analysis of the Washing Machine System with an Automatic Balancer," Trans. of KSME, Vol. 28, No. 8, pp. 1212-1220, 2004.
4. Wlerzba, P., Cao, W., Park, C. W., Park, J. S., and Kim, H. K., "Development of balancer for reduced vibration of washing machine," Proc. of KSPE Spring Conference, pp. 602-607, 1997.
5. Kang, S. K., Lee, J. W., Kim, H. W., Yoo, W. S., and Nho, K. H., "Study on the fluid drag force in ball-balancer for washing machines with experimental method," Proc. of KSME Spring Conference, pp. 39-41, 2010.
6. Uribiola-Soto, L. and Lopez-Parra, M., "Dynamic Performance of the LeBlanc Balancer for Automatic Washing Machines," J. Vib. Acoust., Vol. 133, No. 4, Paper No. 041014, 2011.
7. Jung, C. H., Kim, C. S., and Choi, Y. H., "A dynamic model and numerical study on the liquid balancer used in an automatic washing machine," J. Mech. Sci. Technol., Vol. 22, pp. 1843-1852, 2008.
8. Chen, H. W. and Zhang, Q. J., "Stability analyses of a vertical axis automatic washing machine with a hydraulic balancer," Mech. Mach. Theory, Vol. 46, No. 7, pp. 910-926, 2011.
9. Bae, S., Lee, J. M., Kang, Y. J., Kang, J. S., and Yun, J. R., "Dynamic analysis of an automatic washing machine with a hydraulic balancer," J. Sound Vib., Vol. 257, No. 1, pp. 3-18, 2002.
10. PIDOTECH Inc., "PIAnO (Process Integration, Automation and Optimization) User's Manual, Ver. 3.3," 2011.
11. Forrester, A. I. J., Sobseter, A., and Keane, A. J., "Engineering Design via Surrogate Modeling," John Wiley & Sons, pp. 14-15, 2008.
12. Montgomery, D. C., "Design and Analysis of Experiments," John Wiley & Sons, pp. 347-372, 2005.
13. Fang, X. J., Wang, L. P., Besson, D., and Wiggs, G., "A Practical Robust and Efficient RBF Methmodel Method for Typical Engineering Problems," Proc. of the ASME 2008 Int'l Design Engineering Tech. Conf. Computers Information in Eng. Conf., Vol. 1, pp. 873-882, 2008.
14. Gutmann, H. M., "A Radial Basis Function Method for Global Optimization," J. Global Optim., Vol. 19, pp. 201-227, 2001.
15. Forrester, A. I. J., Sobester, A., and Keane, A. J., "Engineering Design via Surrogate Modeling: A Practical Guide," John Wiley & Sons, pp. 45-49, 2008.
16. Orr, M. J. L., "Introduction to Radial Basis Function Networks," 1996.
17. Baxter, B., "The Interpolation Theory of Radial Basis Functions," Ph.D. Thesis, University of Cambridge, 1992.
18. Kim, J. R. and Choi, D. H., "Enhanced two-point diagonal quadratic approximation methods for design optimization," Comput. Meth. Appl. Mech. Eng., Vol. 197, pp. 846-856, 2008.